

Simulation of point source wetting pattern of subsurface drip irrigation

Wei Wei Yao · Xiao Yi Ma · Juan Li ·
Martin Parkes

Received: 26 April 2010 / Accepted: 22 September 2010 / Published online: 12 October 2010
© Springer-Verlag 2010

Abstract Laboratory experiments and calculations were carried out to analyze the effect of subsurface drip irrigation (SDI) design features on soil wetting patterns for a point source. Experimental and simulated soil wetting patterns, using the SWMS-2D (simulating water movement and solute transport in two-dimensional) Galerkin finite element model, were investigated to maximize the efficiency of water saving. The analysis addressed the influence of water pressure head, back pressure and emitter diameter on wetting patterns. Predictions of water content distributions in the soils made with SWMS-2D were found to be in good agreement with the observed data. Results showed that this model provides confidence that model predictions are not too sensitive to back-pressure effects.

Introduction

Improving agricultural water use efficiency is vitally important in regions that have limited water resources. Subsurface drip irrigation (SDI) can be used to improve irrigation uniformity and water use efficiency in a number of cropping systems by applying a low volume of water to crop root zones. By applying water below the soil surface, water can be conserved by providing water directly to the root zone and reducing evaporative water losses in agricultural systems. SDI has been practiced since ancient

times, including pot irrigation (Bainbridge 2001). With the development of precise irrigation technology, subsurface drip irrigation has progressed from being a novelty employed by researchers to an accepted method of irrigation of field crops, vegetables and fruits (Camp 1998; Singh et al. 2006). Today, SDI offers a strong competitive edge because of its greater water use efficiency compared to other irrigation methods such as flood, furrow, sprinkler and surface irrigation. For low irrigation capacity, the SDI method had the highest grain yield and crop water use index (Fairweather et al. 2003) compared with the low-energy precision application and spray irrigation (Colaizzi et al. 2004). In many parts of the world, especially in arid regions as well as in areas where water is scarce and power is either unavailable or expensive, this irrigation method will be an important technique for irrigation and water conservation.

In subsurface drip irrigation systems, emitters are buried below the soil surface so water seeps from the emitters into the soil and spreads out in the root zone due to capillary forces. Singh and Singh (1978), Camp (1998), and Bhatnagar and Srivastava (2003) found that subsurface drip irrigation methods have high water use efficiency, namely high crop yield per unit amount of applied water. However, the efficiency may be affected by the water application volume and by system design parameters such as the depth or discharge rate and duration of water application, which determine the extent of deep percolation water losses and soil saturation problems. Also, evaporation losses are minimized when the wetting front is kept below the soil surface. Hence, an ability to predict the geometry and water distribution of the wetted zone for different soils and system designs can be very useful for developing guidelines and criteria for optimizing the performance of subsurface drip irrigation systems (Zur 1996).

Communicated by J. Ayars.

W. W. Yao · X. Y. Ma (✉) · J. Li · M. Parkes
Northwest Agriculture and Forest University,
712100 Yangling, Shaanxi, China
e-mail: yao123wei_2002@yahoo.cn

Soil wetting patterns under SDI have been measured and analyzed theoretically by a number of authors, including Philip (1968, 1984), Raats (1971), Cote et al. (2003), Li et al. (2003), Singh et al. (2006), Kandelous et al. (2008, 2010), Gupta et al. (2009) and Siyal and Skaggs (2009), to name only a few. Among these studies, several of the more recent ones (Singh et al. 2006; Kandelous et al. 2008; Gupta et al. 2009; Siyal and Skaggs 2009) have used numerical, analytical and empirical models to simulate soil wetting. For example, Singh and Gupta demonstrated that empirical model simulations of drip irrigation were in agreement with detailed field measurements. Kandelous and Siyal evaluated the accuracy of several approaches used to estimate wetting zone dimensions by comparing their predictions with field and laboratory data.

Nevertheless, there are conflicting accounts regarding the transient nature of emitter flows and their representation, occurring during the initial stages of infiltration. Lazarovitch et al. (2005) explain that the pressure head at a point source outlet increases and becomes positive when an open air discharge of a subsurface source is larger than the soil infiltration capacity. So, a pressure buildup in the soil reduces the pressure difference across the source orifice and, subsequently, decreases the source discharge rate. Such reductions are larger for soils having lower hydraulic conductivity, and the positive pressure in the source vicinity increases rapidly at the beginning of an infiltration event, approaching a final value after only several minutes. They examined flow conditions for emitters with spheres placed at 0.25 m depth in Arava sandy loam and Magal clay loam. Sources with nominal discharges of 4 and 8 l/h were used. For both sources, back pressures increased rapidly during the first 10–15 min and then gradually approached constant values 2 and 3.7 m for the 4 and 8 l/h sources, respectively. Then, for the observed increases in back pressures from 0 to 3.7 m, the discharge rate dropped from 2.22 to 1.73 10^{-3} l/s. Existence of this phenomenon is also supported by the finding of Cote et al. (2003) that for silt and the silty clay loams, a discharge rate 1.65 l/h was too high relative to the intake rate of these soils, resulting in failure of their numerical model.

In contrary findings, Gupta et al. (2009) have shown that in a comparison of porous clay pipe emissions either in free air or installed below ground, emission rates are initially higher for the in situ pipes. For pipes embedded in the soil, emission rate is judged to be a function of soil texture and applied hydraulic head. For a given soil texture, as the applied hydraulic head in the pipe increases, the water content in the vicinity of the pipe becomes higher, and the effect of the capillary forces on the emission rate of the pipe decreases. They found higher stable in-situ emission rates for open air emission rates up to 2.7 l/m/h at 2 m

hydraulic head. In their examination of subsurface drip irrigation using porous clay pipe, Siyal and Skaggs (2009) reported that their computer simulations with HYDRUS (2D/3D) showed that as pressure head in the irrigation pipe was increased, the size of the wetted zone also increased, with no apparent back-pressure effects, nor capillary effects.

Surfacing problems can occur with subsurface drip installations when emitter flow rates exceed local infiltration rates. Clay textures promote the phenomenon, which is seen as an impaired drainage problem. In one instance on sandy loam soils with drip lines emitting 4 l/h at 0.6 m depth, no surfacing occurred. By comparison, 2 l/h lines at 0.75 m in clay loam did cause surfacing. If there is low saturated hydraulic conductivity, with subsurface drip the three-dimensional wetted area pushes water through paths of least resistance. This is commonly the newly disturbed soil above the drip line.

Several models are often used to simulate water flow, such as HYDRUS, SWMS-2D, APRI (Zhou et al. 2007). Estimates of average relative error between simulated and measured soil water content are about 10% for the SWMS model and from 11 to 29% for the HYDRUS-2D model (Zhou et al. 2007), indicating that the two models perform well in simulating soil water dynamic under the SDI. But the SWMS model is simpler for modeling soil water dynamics compared with HYDRUS. So, the objective of this study was to compare measurements with simulated soil wetting under SDI from a point source using SWMS-2D and to investigate the sensitivity of the model to back-pressure effects on emitter discharge rates.

Model development

Theoretical considerations

Since all experiments used only one emitter as the point source of water, water movement during infiltration could be considered an axi-symmetrical process. The partial differential equation governing the flow of water from a point source through variably unsaturated media can be written as follows:

$$\frac{\partial \theta}{\partial t} = \frac{1}{r} \frac{\partial}{\partial r} \left[K(h) \frac{\partial h}{\partial r} \right] + \frac{\partial}{\partial z} \left[K(h) \frac{\partial h}{\partial z} \right] - \frac{\partial K(h)}{\partial z} \quad (1)$$

where θ is the volumetric water content (cm^3/cm^3); $K(h)$ is the hydraulic conductivity of the point source (cm/min); h is the total potential head (cm); z is the depth from the soil surface (cm), taken positive upward; r is the horizontal distance (cm); and t is time (min).

The computer code SWMS-2D (Simunek et al. 1995) solves Eq. 1 using a finite element approximation. The

initial and boundary conditions of the system are as follows:

$$h(r, z, t) = h_0(r, z), (0 \leq r \leq R, 0 \leq z \leq Z, t = 0);$$

on ABDCEA in Fig. 1.

$$\frac{\partial \theta}{\partial t} = \frac{\partial}{\partial r} \left[K(h) \frac{\partial h}{\partial r} \right] + \frac{1}{r} K(h) \frac{\partial h}{\partial r} + \frac{\partial}{\partial z} \left[K(h) \frac{\partial h}{\partial z} \right] - \frac{\partial K(h)}{\partial z} + Q \quad (2)$$

$$Q = a(H + h_e - h_s)^b \text{ at the point E in Fig. 1} \quad (3)$$

where Q is the flow rate of the pipe (ml/min); H is the hydraulic head inside the pipe (cm); h_s is the back pressure created by emitter discharge exceeding infiltration rate; h_e is the capillary head of soil in the flow domain (cm); a and b are shape parameters that depend on the d (emitter's diameter) as well as the pipe material. In this experiment, $a = 6.8169d^{2.3936}$, $b = 0.716 - 0.2138d$ (Ma et al. 2006).

The boundary conditions are specified along the boundary geometry along with values of the dependent variables or their derivative normal to the boundary.

$$t > 0, \frac{\partial h}{\partial z} = 0, \text{ along AB (no evaporation at soil surface);} \quad (4)$$

$$t > 0, \frac{\partial h}{\partial r} = 0, \text{ along AE, EC, BD (zero flux boundaries);} \quad (5)$$

$$t > 0, h(r, d, t) = h_0, \text{ along CD} \quad (6)$$

(constant head at the base of the flow domain);

where h_0 is the initial water content of the soil in the soil bin and d is the depth of the flow domain, with reference to point A.

Determination of soil hydraulic parameters

Soil water characteristic data were fitted to the Van Genuchten (1980) retention model using the computer program developed by van Genuchten et al. (1991). The van Genuchten model is as follows:

$$\theta(h) = \begin{cases} \theta_r + \frac{\theta_s - \theta_r}{(1 + |\alpha h|^n)^m} & h < 0 \\ \theta_s & h \geq 0 \end{cases} \quad (7)$$

$$\theta_s = 1 - \frac{\rho_b}{2.65} \quad (8)$$

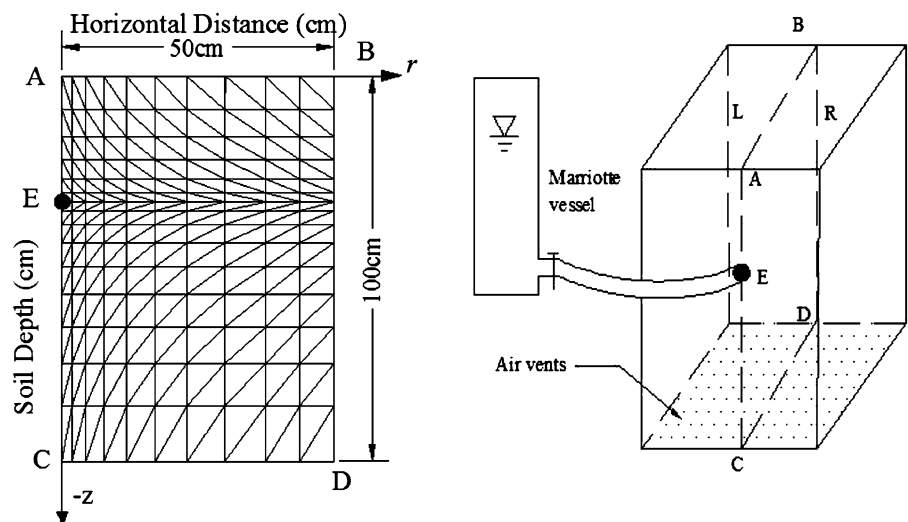
$$K(h) = K_s S_e^l \left[1 - (1 - S_e^{1/m})^m \right]^2 \quad (9)$$

where θ_r and θ_s are the residual and saturated water contents ($\text{cm}^3 \text{cm}^{-3}$), respectively; ρ_b is the bulk density; K_s is the saturated hydraulic conductivity (cm/min); α is an empirical constant that is inversely related to the air-entry pressure value (cm^{-1}); n is an empirical parameter related to the pore-size distribution; l is an empirical shape parameter; $m = 1 - 1/n$; and S_e is the effective saturation given by the following equation:

$$S_e = \frac{\theta - \theta_r}{\theta_s - \theta_r} \quad (10)$$

The water retention curve (Fan 2008) is one of the important factors to represent the soil characteristics. In order to get the water retention curve, a centrifugal machine (SCR-20) was used. Firstly, saturated soil samples were put into it. Then, various parameters were set such as temperature and rotational speeds of 900, 1,700, 2,200, 2,800, 3,100, 5,300, 6,900 and 8,100 rpm, respectively, being maintained for 1 h. Then, soil water content could be

Fig. 1 Finite element representation and SDI measuring device. L (left side), R (right side)



measured for each rotational speed, while the capillary head could be calculated as follows:

$$\phi_m = 1.118 \times 10^{-5} \times R \times (\text{rpm})^2 \quad (11)$$

where ϕ_m is the capillary head; R is 9.8; and rpm is the rotational speed.

The observed and fitted water retention curves for the experimental soils are shown in Fig. 2. Hydraulic properties of the soils and parameters of the van Genuchten model used for simulating the soil water distribution are given in Table 1.

Testing the model

Laboratory setup

Medium loam and sandy loam soils from the Loess Plateau, China, were used for the experiments. The soil was collected from the 20–60 cm depth of a field just after winter wheat was harvested. A large volume of soil was obtained and air-dried for the same time. The soil materials were passed through a screen of 2 mm before being packed into the box. In order to ensure the experimental bulk density attained a real field value, some water was added to the dry soil and mixed with the soil before filling the soil bin. Loading and compaction of soil in the bin was done in 5-cm layers to obtain a homogeneous soil profile. To

maintain zero evaporation, the soil was covered with a polyethylene sheet.

Only one side of the vertical cross-section was simulated, with the point source on the side of an otherwise rectangular computational domain. The flow domain was discretized with 342 nodes and 380 triangular elements, using smaller spacings close to the point source (Fig. 1). A soil bin was designed and fabricated to study the effect of soil texture on the emission characteristics of a trickle emitter. Figure 1 illustrates the laboratory setup for the experiments. The soil bin, made of 10-mm-thick transparent acrylic material, was 100 cm long, 100 cm deep and 50 cm wide. A drainpipe was installed at one side of the soil bin at a depth of 25 or 40 cm below the soil surface with the 5-mm-diameter hole. The bottom of the soil bin had many 2-mm parallel air vents for ventilation, and at both sides of the soil bin, there were side holes (20 mm) for soil unloading. Before the mixed soil was put into the soil bin, on both sides of the soil bin, transparent adhesive tape was placed on to prevent the soil falling out of the box. A Mariotte vessel was used to maintain a constant hydraulic head (60 and 150 cm for each soil type).

Laboratory experiment

An experiment to measure soil wetting patterns was carried out in the laboratory soil bin. Eight irrigation arrangements were investigated, as described by case I to case VIII in

Fig. 2 Observed (black diamond) and fitted (hyphen) water retention curves of the experimental (a, b) medium loam soils and (c, d) sandy loam soils using van Genuchten (1980) model

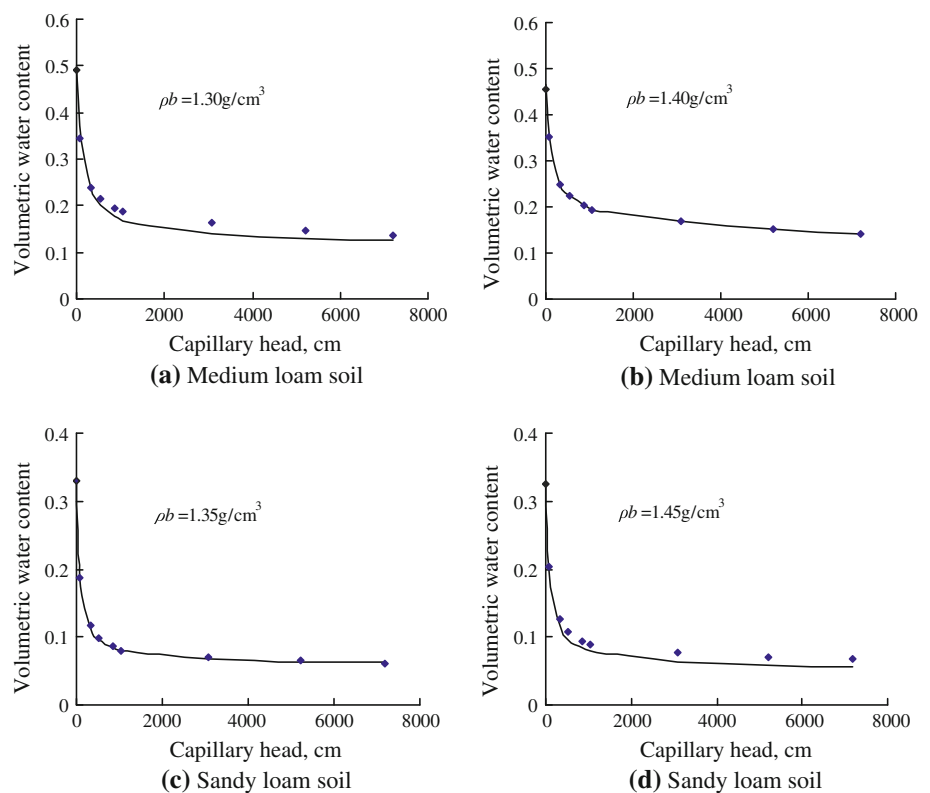


Table 1 Results of fitting VG model parameters

Soil type	Bulk density (g/cm ³)	θ_r	θ_s	α	n	l	K_s (min/cm)
Medium loam soil	$\rho_b = 1.3$	0.1185	0.509	0.0322	1.32860	0.5	0.491
Medium loam soil	$\rho_b = 1.4$	0.0085	0.472	0.05099	1.16753	0.5	0.513
Sandy loam soil	$\rho_b = 1.35$	0.0698	0.491	0.03135	1.80175	0.5	1.248
Sandy loam soil	$\rho_b = 1.45$	0.0491	0.453	0.04172	1.81943	0.5	0.435

Table 2 SDI experiment to investigate the accuracy of SWMS model

Case	Soil type	Emitter diameter (mm)	Installation depth (cm)	Hydraulic head (cm)	Bulk density (g/cm ³)	Initial water content (cm ³ /cm ³)	Volume applied (l)
I	Medium loam soil	0.6	25	60	1.3	0.153	14.7
II		1.2	40	60	1.3	0.184	29.5
III		0.6	25	150	1.4	0.198	29.5
IV		1.2	40	150	1.4	0.165	14.7
V	Sandy loam soil	0.6	40	150	1.35	0.111	29.5
VI		1.2	25	150	1.35	0.134	14.7
VII		0.6	40	60	1.45	0.144	14.7
VIII		1.2	25	60	1.45	0.120	29.5

Table 2. Either 14.7 or 29.5 l of water was applied during irrigation at either 0.25 or 0.4 m depth, using either an inside diameter 0.6 or 1.2-mm emitter (outside diameter 5 mm). In order to eliminate preferential flow along the wall of the box, the emitter was inserted into the soils by about 20 mm. Around each emitter, after half the water had been applied and all water had been applied, the left side transparent adhesive tape was pulled off and measurements were taken. “The sampling layout had horizontal and vertical intervals of 10 cm, starting at 10 cm below the surface and continuing every 10 cm to a final depth of 90 cm (Fig. 3)”. A tube of 50 cm length and 2 cm diameter was driven horizontally into the left-hand side of the soil bin at each of the sampling points to intersect the ABDC plane in Fig. 1. Soil cores were obtained from the tip of the sampling tool to represent the desired sampling locations. About 10 gram of the soil sample was used to measure the water content (Fig. 3).

The soil sampling time for each experiment was approximately 15 min. Soil samples were collected by soil drill, and the volume voided by the samples was re-packed with soil in order to keep the symmetry of the wetted zone. To maintain the experimental conditions, the soil water sampling was undertaken from the left side of the soil bin after half the water had infiltrated and from the right side after all the water had infiltrated. In cases I to IV, the procedure was repeated with two boxes to ensure consistency in the soil water sampling procedure. It was assumed that the soil in the bin was homogeneous and the

distribution of water in the soil was symmetrical. The soil water contents of the samples were determined by recording the weight loss of the samples after oven drying at 105°C for 24 h. Measurements of soil water content were obtained throughout the irrigation process, and measurements normally took up to 7 h to complete for each experiment. Simulations of case II, case V and case VIII were determined for comparison with measured data.

The simulation of soil wetting patterns by SWMS-2D and the processing of data included the following steps: (1) VG model parameters were set along with other chemical solute parameters. (2) Nodes and triangular elements were created in a grid file. (3) The initial and boundary conditions were set. (4) The SWMS-2D program was run. (5) Nodes were chosen whose positions were the same as those measured in the laboratory experiment, and the nodes' soil water content values were compared for the simulation and laboratory experiment (Table 3). Since the nodes used in SWMS-2D were many more than those measured in the laboratory, MATLAB software was used to draw the contour lines to represent wetting (Fig. 3).

The agreement of the SWMS-2D simulations with the measured data was quantified by three statistical measures, the mean absolute error (MAE), root mean squared error (RMSE) and percent bias (PBIAS). These parameters are defined as follows:

$$\text{MAE} = \frac{\sum_{i=1}^n |Y_i^{\text{sim}} - Y_i^{\text{obs}}|}{n * Y_i^{\text{obs}}} \times 100\% \quad (12)$$

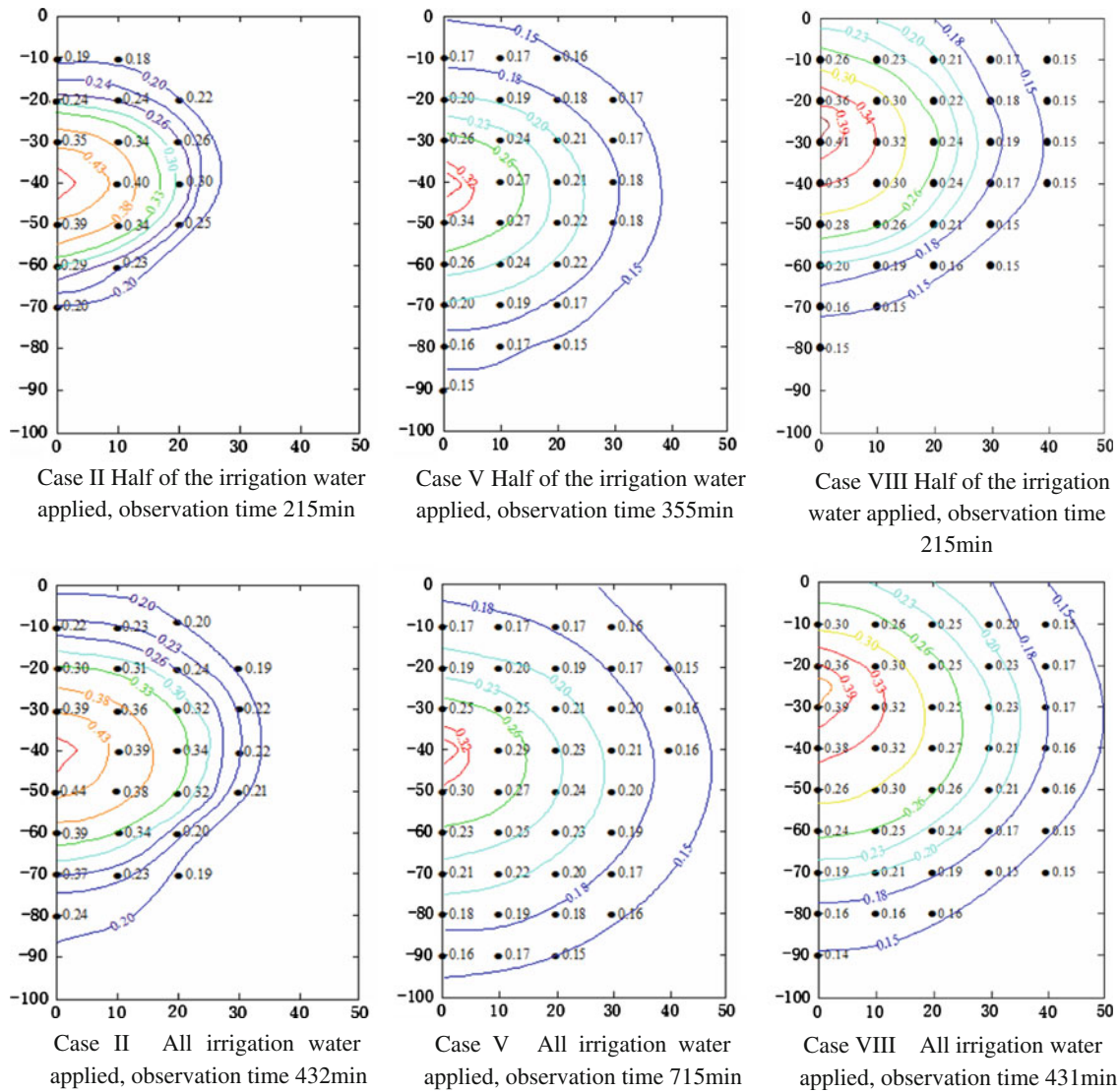


Fig. 3 Comparison of simulated and observed soil water contents (volumetric water content)

Table 3 Parameters used in SWMS-2D simulations

Case	Soil type	Diameter (mm)	Installation depth (cm)	Pressure head (cm)	Bulk density (g/cm ³)	Initial water content (cm ³ /cm ³)	Volume applied (l)
I	Medium loam soil, Sandy loam soil	0.6, 1.2	35	60, 150	1.30, 1.35	0.184; 0.134	22.5
II	Medium loam soil, Sandy loam soil	0.9	35	100	1.30, 1.35	0.153, 0.184, 0.215; 0.111, 0.134, 0.156	22.5
III	Sandy loam soil	0.9	35	100	1.35, 1.45	0.134, 0.144	22.5
IV	Medium loam soil, Sandy loam soil	0.9	25, 35, 45	100	1.30, 1.35	0.184; 0.134	22.5

$$RMSE = \sqrt{\frac{1}{n-1} \sum_{i=1}^n (Y_i^{sim} - Y_i^{obs})^2}, \text{ for } i = 1, 2, \dots, n \quad (13)$$

$$PBIAS = \left[\frac{\sum_{i=1}^n (Y_i^{obs} - Y_i^{sim}) * (100)}{\sum_{i=1}^n (Y_i^{obs})} \right] \quad (14)$$

where n is the total number of data points in each case, Y_i^{sim} is the i th simulated data point and Y_i^{obs} is the i th observed data. The MAE can potentially identify the presence of bias. The RMSE gives an overall measure of the amount by which the data differ from the model predictions, whereas

PBIAS is the deviation of data being evaluated, expressed as a percentage. If the PBIAS was $<\pm 10\%$, the values of PBIAS would be considered as within a very good range (Moriassi et al. 2007).

Average in situ emitter discharge rates were determined, based on measurements by Mariotte vessel, for the four soil textures with bulk density ranging from 1.3 to 1.45 g/cm³. Discharge rates in air for the same values of hydraulic head were also measured to represent values without back pressure. Free discharge and flow into packed soil was also determined for a 0.9-mm id emitter. Soil water contents for different hydraulic heads and emitter diameters were predicted for a number of cases identified in Table 3.

Results and discussion

The comparison of measured and simulated wetting pattern data is shown in Fig. 3. The observed data are represented by grid points, while predictions are shown using water contents as contour lines. In checking the consistency of the soil water sampling technique, for the first 4 cases, measurements of soil water at the sampling points in the ABDC plane agree within 2%. Values of MAE, RMSE and the PBIAS for observed and predicted water contents are given in Table 4.

It is clear from Table 4 and the contour plots shown in Fig. 3 that in general, the predicted soil water distribution fits well with the experimental data, though a few plots near the point source did not have good agreement. MAE values are indicative of good model performance. The average value of MAE was only 5.6% across all treatments, which is better than the results of Siyal and Skaggs (2009). The average value of RMSE was 0.016, which corresponds to a very small spread in the data, and the result is better than results presented by Skaggs et al. (2004). The absolute value of PBIAS varied from 0.02 to 9.65, which represents a very good range (Moriassi et al. 2007).

A comparison of the discharge rates in situ and in air for different emitter diameter, hydraulic head and total volume applied is given in Table 5. A back-pressure effect is evident.

Simulated effects of pressure head and the emitter diameter

Figure 4 shows predicted soil water content for different hydraulic heads and emitter diameters. From Fig. 4a and b along with Fig. 4e and f, it is apparent that the wetted soil volume increases a little or not as the emitter diameter was increased from 0.6 to 1.2 mm. Examining Fig. 4b and c together with Fig. 4f and g, it can be seen then that the wetted soil volume remained unchanged as the hydraulic head increased from 60 to 150 cm. This result differs from that of Siyal and Skaggs (2009) who observed no back-pressure effects. However, it is similar to the results of Lazarovitch et al. (2005). Comparing the results of Siyal and Skaggs (2009) and the results determined by SWMS-2D, it appears that until the hydraulic head reaches a limiting level at which back pressure develops, the wetted zone will increase with increasing hydraulic head. At this point, the discharge rate becomes too high relative to the intake rate of these soils and back pressure inhibits flow (Cote et al. 2003). Nevertheless, agreement of model and measurements is good, even without the system-dependent boundary condition introduced by Lazarovitch et al. (2005), considering source properties, inlet pressure and effects of the soil hydraulic properties on calculated sub-surface emitter flow.

Basically, even back-pressure effects have been observed, the agreement between measurement and prediction gives confidence to accept the model predictions. It

Table 5 Relationship between water discharges in air and in soil

Emitter's diameter (mm)	Hydraulic head (cm)	Emitter discharges in the air (l/h)	Emitter discharge in the soil (l/h)
0.6	95	1.73	1.67
0.9	125	3.90	3.60
0.9	135	4.06	3.60
0.9	145	4.22	3.60
1.2	185	6.77	6.20
1.2	95	5.00	4.23

Table 4 Correlation between simulated and measured soil water contents

No.	Volume applied (l)	Evaluation statistic			Volume applied (l)	Evaluation statistic		
		MAE (%)	RMSE	PBIAS		MAE (%)	RMSE	PBIAS
Case II	14.8	8.0	0.024	-3.40	29.5	6.5	0.023	-3.59
Case V	14.8	4.4	0.011	0.02	29.5	5.6	0.013	-1.30
Case VIII	14.8	4.1	0.013	3.19	29.5	4.9	0.014	9.65

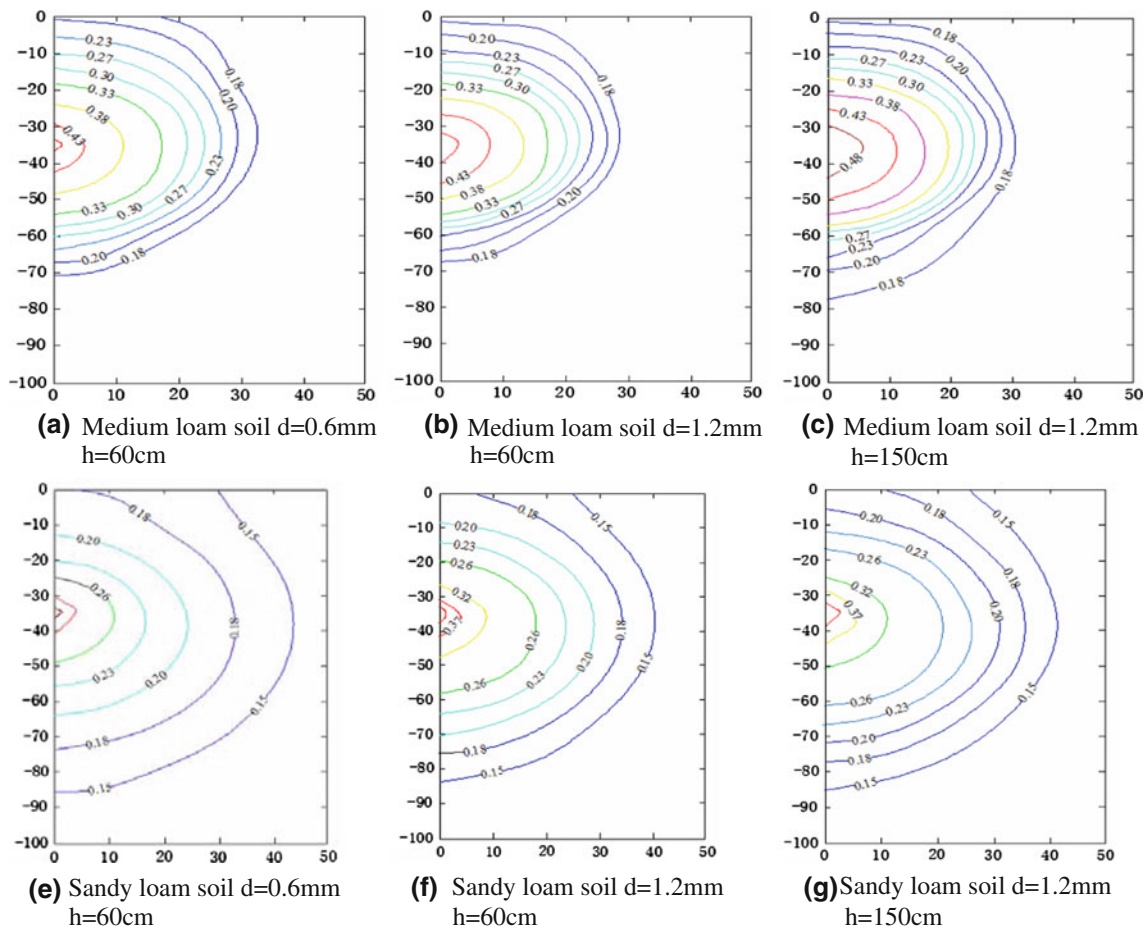


Fig. 4 Effects of different pressure head and diameter on soil water distribution

is important that emitter flows are matched to soil types, so that back-pressure effects are avoided. Low discharge rate is not to be advised to avoid blockage, but high flows will induce back pressures.

Conclusions

The SWMS-2D software was used to simulate soil wetted depth and width under SDI for a point source of water application. The results of laboratory experiments indicated that the simulated model values of soil water distribution were not different from observed ones. Differences of emitter discharge rates determined in situ and in air showed that back-pressure effects were evident in this study, but this did not influence agreement between model predictions and measurements.

Acknowledgments We are grateful for financial support from Chinese National Natural Science Foundation (No. 50879072), 2006BAD11B04 Project and BJRC-2009-001 Project.

References

- Bainbridge DA (2001) Buried clay pot irrigation: a little known but very efficient traditional method of irrigation. *Agric Water Manage* 48(2):79–88
- Bhatnagar PR, Srivastava RC (2003) Gravity-fed drip irrigation system for hilly terraces of the northwest Himalayas. *Irrig Sci* 21:151–157
- Camp CR (1998) Subsurface drip irrigation: a review. *Trans ASAE* 41(5):1353–1367
- Colaizzi PD, Schneider AD, Evett SR, Howell TA (2004) Comparison of SDI, LEPA, and spray irrigation performance for grain sorghum. *Trans ASAE* 47(5):1477–1492
- Cote CM, Bristow KL, Charlesworth PB, Cook FJ, Thorburn PJ (2003) Analysis of soil wetting and solute transport in subsurface trickle irrigation. *Irrig Sci* 22:143–156
- Fairweather H, Austin N, Hope M (2003) Water use efficiency: an information package. NPSI Irrigation Insights 5. p 67
- Fan YW (2008) Study on numerical simulation of interference infiltration characteristic in film hole irrigation. Master's degree thesis, Northwest A & F University, Shaanxi, China
- Gupta AD, Babel MS, Ashrafi S (2009) Effect of soil texture on the emission characteristics of porous clay pipe for subsurface irrigation. *Irrig Sci* 27:201–208
- Kandelous MM, Simunek J (2010) Comparison of numerical, analytical, and empirical models to estimate wetting patterns

- for surface and subsurface drip irrigation. *Irrig Sci*. doi:10.1007/s00271-009-0205-9
- Kandelous MM, Liaghat A, Abbasi F (2008) Estimation of soil moisture pattern in subsurface drip irrigation using dimensional analysis method. *J Agri Sci* 39(2):371–378 (in Persian)
- Lazarovitch NS, Simunek J, Shani U (2005) System-dependent boundary condition for water flow from subsurface source. *Soil Sci Soc Am J* 69(1):46–50
- Li J, Zhang J, Ren L (2003) Water and nitrogen distribution as affected by fertigation of ammonium nitrate from a point source. *Irrig Sci* 22(1):19–30
- Ma XY, Xie JB, Kang YH (2006) Finite element simulation study on soil water movement under gravity subsurface drip irrigation. *Irrig Drainage* 25(6):5–10
- Moriasi DN, Arnold JG, van Liew MW, Bingner RL, Harmel RD, Veith TL (2007) Model evaluation guidelines for systematic quantification of accuracy in watershed simulations. *Trans ASABE* 50:885–900
- Philip JR (1968) Steady infiltration from buried point sources and spherical cavities. *Water Resour Res* 4:1039–1047
- Philip JR (1984) Travel times from buried and surface infiltration point sources. *Water Resour Res* 20:990–994
- Raats PAC (1971) Steady infiltration from point sources, cavities and basins. *Soil Sci Soc Am Proc* 35:689–694
- Simunek J, Huang K, Genuchten MTV (1995) The SWMS-2D code for simulating water flow and solute transport in two-dimensional variably-saturated media, Version 1.0, Riverside, California
- Singh SD, Singh P (1978) Value of drip irrigation compared with conventional irrigation for vegetable production in a hot arid climate. *Agron J* 70:945–947
- Singh DK, Rajput TBS, Singh DK, Sikarwar HS, Sahoo RN, Ahmad T (2006) Simulation of soil wetting pattern with subsurface drip irrigation from line source. *Agri Water Manag* 83:130–134
- Siyal AA, Skaggs TH (2009) Measured and simulated soil wetting patterns under porous clay pipe sub-surface irrigation. *Agric Water Manage* 96:893–904
- Skaggs TH, Trout TJ, Simunek J, Shouse PJ (2004) Comparison of HYDRUS-2D simulations of drip irrigation with experimental observations. *Irrig Drainage ASCE* 130:4 (304)
- Van Genuchten MT (1980) A closed-form equation for predicting the hydraulic conductivity of unsaturated soils. *Soil Sci Soc Am Proc* 44:892–898
- Van Genuchten MT, Leij FJ, Yates SR (1991) The RETC code for quantifying the hydraulic functions of unsaturated soils, Research Report No. EPA/600/2-91/065, US Salinity Laboratory, US Department of Agriculture, Agricultural Research Service, Riverside
- Zhou QY, Kang SZ, Zhang L (2007) Comparison of APRI and Hydrus-2D models to simulate soil water dynamics in a vineyard under alternate partial root zone drip irrigation. *Plant Soil* 291:211–223
- Zur B (1996) Wetted soil volume as a design objective in trickle irrigation. *Irrig Sci* 16:101–105